GeCat 2014: Advances and prospects in heterogeneous catalysis

Uranium (VI) adsorption on synthesized 4A and P1 zeolites: Equilibrium, kinetic, and thermodynamic studies

Adsorption de l'uranium (VI) sur des zéolithes de synthèse 4A and P1 : équilibre, cinétique et études thermodynamiques

Mahfoud Barkat [a], Djamel Nibou [b,*], Samira Amokrane [b], Salah Chegrouche [a], Abdelhamid Mellah [a]

[a] Centre de recherche nucléaire de Draria, Commissariat à l'énergie atomique, 43, Draria, Alger, Algeria
[b] Laboratoire de technologie des matériaux, faculté de génie mécanique et génie des procédés, Université des sciences et de la technologie Houari-Boumediene, BP 32, El-Alia, Bab-Ezzouar, Alger, Algeria

ARTICLE INFO

ABSTRACT

The present work deals with the investigation of the use of synthesized 4A and P1 zeolites in the adsorption of uranium (VI) ions from liquid effluents (with initial concentrations of 100, 85 and 80 mg·L^{-1}). Batch experiments were performed and the effects of temperature, solid–liquid ratio, pH and initial UO_2^{2+} ion concentration were studied, and the optimal parameters were determined. The kinetic and thermodynamic aspects of the process as well as the diffusion mechanism have been studied. The obtained results showed that 4A and P1 zeolites are very effective adsorbents.

© 2014 Académie des sciences. Published by Elsevier Masson SAS. All rights reserved.

RÉSUMÉ

Le présent travail traite l'utilisation des zéolithes de synthèse de types 4A et P1 dans l'adsorption des ions d'uranium (VI) à partir des effluents liquides (avec des concentrations de 100, 85 et 80 mg·L^{-1}). Les expériences ont été réalisées en *batch* et les paramètres optimaux ont été déterminés en étudiant les effets de température, du rapport solide–liquide, du pH et de la concentration des ions uranyles. Des études de cinétique, de thermodynamique et de diffusion ont été aussi réalisées. Les résultats obtenus ont montré que les zéolites 4A et P1 sont des adsorbants efficaces.

© 2014 Académie des sciences. Publié par Elsevier Masson SAS. Tous droits réservés.

* Corresponding author.
  E-mail address: dnibou@yahoo.fr (D. Nibou).

1. Introduction

The adsorption of UO_2^{2+} ions is a process that has recently found many applications in the treatment of the effluents generated in the nuclear industry. The toxicity of these radioactive wastes has been recognized ever since the dawn of nuclear industry. The issue of the waste management represents a great challenge, as the negative impact on both the human health and on the environment is very serious. The lowest standard radioactive waste is fixed to 5 ppm [1,2]. In this respect, many adsorbents have been developed and proposed to deal with these wastes, such as zeolites, porous silica, activated carbon, clay, and resins [3–7]. Besides their application in the nuclear industry, these adsorbents play an important role in the industrial field and primarily those related to the environment; they have also been widely used in the petrochemical synthesis and oil refining [8,9], other diverse applications have significantly increased lately.

Among all these porous materials, the aluminosilicate- and aluminophosphate-based catalysts and their derivatives have, by far, the best technological impact due to their variety, their catalytic activity, and their behaviour as ion exchangers as well as their selective adsorption property. A-Type zeolites are commonly used as dryers in the toxic gases, purification processes [10], while those of faujasite Y and ZSM-5 types are preferred in the petrochemical field and residual oil selective catalytic cracking. However, both of these adsorbents are used in the depollution processes by adsorption/separation [11].

The zeolites are generally prepared under a hydrothermal procedure [12,13] starting from a gel whose basic constituents are silicon, aluminium, a mineralizing agent (hydroxide ion or fluoride media), and an organic template. The first artificial zeolite was synthesized according to the sequences observed in nature, and since then, this synthesis has been constantly improved in order to obtain new structures and a new shape and size-selective properties [14].

This work aims at using two aluminosilicate-types, namely 4A and P1, in the adsorption of UO_2^{2+} ions from synthetic and genuine solutions. 4A zeolite has a cubic structure with LTA-type ($Na_{12}Al_{12}Si_{12}O_{48}$) and having an aperture of 4×4 Å, while P1 has a monoclinic structure with GIS type ($Na_4Al_8Si_8O_{32}$) and an aperture of 4.5×3.1 Å [15].

We have carried out a treatment process based on both exchange reactions and adsorption. Many parameters related to these unit operations have been studied, such as temperature, solid–liquid ratio, pH, and uranyl ions concentration. Besides the kinetics, the equilibrium and the thermodynamics aspects, and as originality, we have dealt with the UO_2^{2+} ion diffusion onto the 4A and P1 zeolites. The results obtained confirmed the effectiveness of both zeolites we synthesized in nuclear waste disposal.

2. Material and method

2.1. 4A and P1 zeolites synthesis and characterization

The process used in this work for the preparation of our zeolites was hydrothermal crystallization as reported in [1,2]. We used aluminium isopropoxide ($Al[OCH(CH_3)_2]_3$ from Fluka) as a new alumina source, fumed silica (from Fluka) and sodium hydroxide (from Prolabo). The mixture was kept under mixing until the formation of a homogenous gel. The overall synthesis mixture was then placed into a stainless steel Teflon lined autoclave. The crystallization occurred on the one hand at a temperature of 90 °C during 72 h without maturation for the preparation of zeolite 4A and on the other hand at temperature of 100 °C during 24 h with maturation for the preparation of zeolite P1. After cooling, the products were filtered, washed many times with distilled water and eventually dried at 100 °C for 6 h.

The identification of the products was carried out by X-ray diffraction (Philips PW 1800, using Cu Kα radiation, with a 2θ scan range from 5 to 50°). The XRD patterns obtained were compared with those of reference [16] and identified as the 4A Fig. 1a and P1 Fig. 2a zeolite phases.

Surface morphology was observed by using scanning electronic microscopy (Philips XL 30) equipped with energy-dispersive spectrometry for chemical analysis. The zeolites were coated with a thin film of carbon. It was found that the crystallites of 4A and P1 form as fine cubic particles with an average size of 3.5 and 1.5 μm, respectively. The anhydrous chemical compositions were also determined and the formulas obtained for both zeolites are respectively $Na_{0.1804}Si_{0.4118}Al_{0.4007}O_2$ and $Na_{0.1192}Si_{0.5424}Al_{0.3383}O_2$. The zeolite surface area was determined by the BET method and the results found ranged between 260 to 350 $m^2 \cdot g^{-1}$ and porous volumes of 0.16 to 0.17 $mL \cdot g^{-1}$ for P1 and 4A, respectively. An XRD study was carried out on samples after UO_2^{2+} ion exchange; it was shown that the crystallinity of the zeolites remained stable even at low pH as it is illustrated in Fig. 1b and Fig. 2b. Comparing the relative intensities of the planes corresponding to 4A and P1 zeolites before and after UO_2^{2+} ion exchange, no significant change has been observed either in the position of the most intense peaks nor in their crystallinity. In another study [1] about UO_2^{2+} removal onto synthetic NaA zeolite, a shift of inter reticular distance (d_{222}) of about 0.04 Å was observed and diffraction planes (640) and (840) had completely disappeared due to the presence of uranium metal.

2.2. Used reagents

An amount of 1 $g \cdot L^{-1}$ uranyl nitrate stock solution was prepared by dissolving an appropriate amount of uranyl nitrate hexa-hydrated salt ($UO_2(NO_3)_2 \cdot 6$ H_2O) in distilled water with 1 mL of concentrated nitric acid. The experiments were carried out in batch, in a set of 200-cm^3 screw-cap conical flasks containing zeolites. A fixed volume of uranyl nitrate solution with different initial uranium concentrations ranging from 5 to 100 $mg \cdot L^{-1}$ is introduced into each flask. The mixture was carefully stirred by means of a rotary shaker at a rate of 350 rpm. Both solid and liquid phases were separated by centrifugal action and the filtrates collected were analyzed by UV–visible spectroscopy. Arsenazo-III was used to complex uranium species [17].
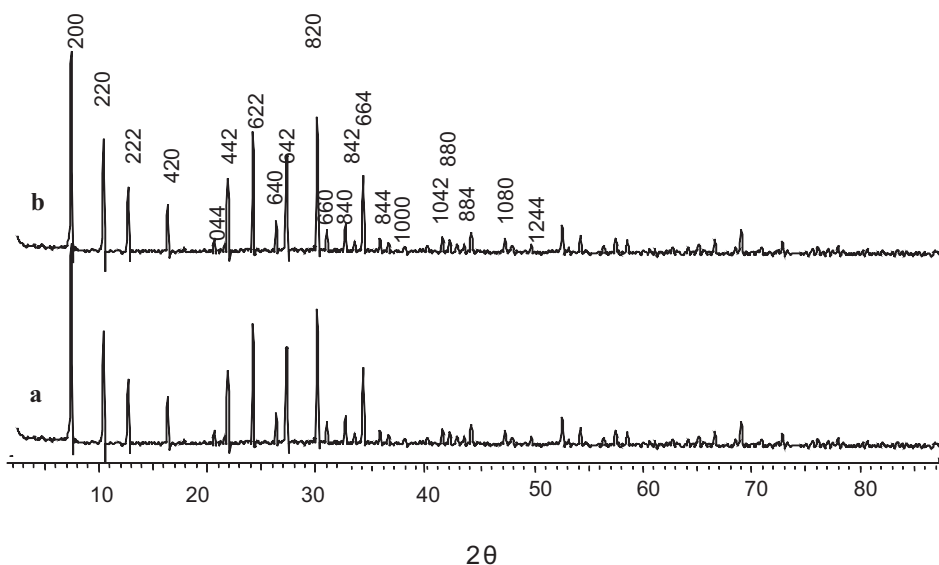
Fig. 1. XRD patterns of zeolites (a) 4A and (b) exchanged UO$_2$ 4A at pH = 2.

2.3. Parametric study

This part was aimed at studying of uranium adsorption onto 4A and P1 zeolites. It consists in investigating the influence of the following parameters: the contact time, the pH, the uranyl initial concentration and the temperature on the adsorption process yield. The instantaneous adsorbed uranium quantity in mg·g^{-1} is determined by the equation:

$$q_t = (C_0 - C_t) = V/m \tag{1}$$

where C_0 and C_t are the uranyl initial concentrations at time $t = 0$ and time t in mg·L^{-1}. V is the solution volume of

the sample in ml and m is the zeolite amount used in g (Table 1). The percent adsorption was determined through the expression:

$$R(\%) = [(C_0 - C_t)/C_0] \times 100 \tag{2}$$

2.4. Kinetic studies

In order to understand the mechanism of the uranium adsorption process onto 4A and P1 zeolites, three main kinetic models were tested as reported by Nibou et al. [1], the pseudo first-order and pseudo second-order ones and the intraparticle diffusion one.
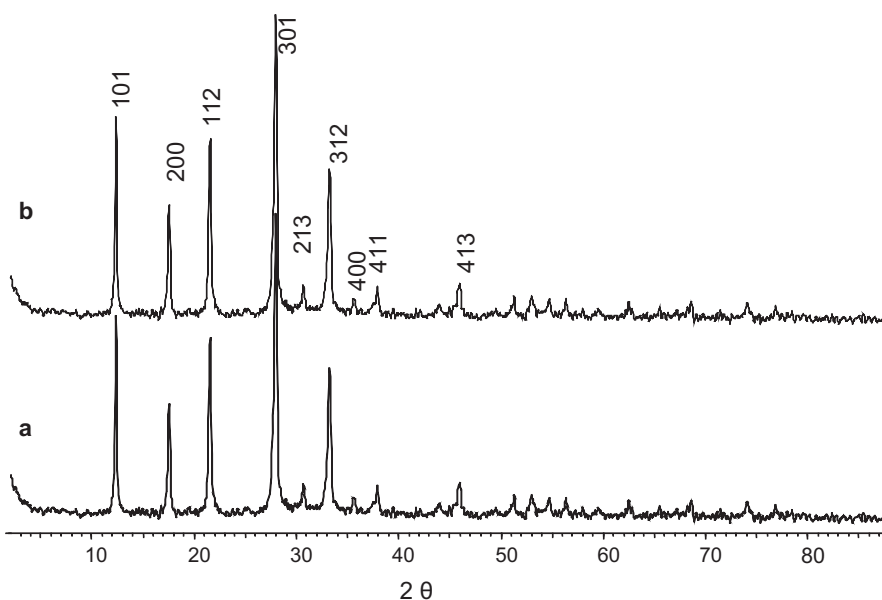

Fig. 2. XRD patterns of zeolites (a) P1, (b) exchanged UO$_2$P1 at pH = 2.5.

Table 1
Adsorption capacity of UO_2^{2+} onto zeolites 4A and P1 at time t.

UO_2^{2+} initial concentration (mg·L^{-1})	5	10	20	30	50	60	80	100
Adsorption capacity (mg·g^{-1}) 4A	8.5	12.4	15.2	18	21	21.6	25.6	32
Adsorption capacity (mg·g^{-1}) P1	8.3	16	31.2	35.4	53	62.4	80	100

2.5. Equilibrium isotherms

The Freundlich model is a purely empirical formula. The adsorption takes place in multilayer mode where the amount of adsorbed solute at equilibrium is related to the uranyl ion concentration at equilibrium by the equation:

$$q_e = K_f \, C_e^{1/n} \tag{3}$$

According to the Langmuir isotherm, the adsorption process occurs on the active sites of the material, and once the uranyl ions fill these sites, the adsorption stops after proceeding in monolayer mode, and can be modeled by the following equation:

$$q_e = Q_0 \, b \, C_e / (1 + b \, C_e) \tag{4}$$

The last investigated isotherm is the so-called Dubinin–Raduchkevitch (D–R) isotherm; it is more general than the Langmuir one, as in the former, we do not assume the homogeneity of the material surface or a constant adsorption potential. The D–R isotherm is represented by the following relation:

$$\ln q_e = \ln q_{max} - K_{ads} \, \varepsilon^2 \tag{5}$$

where q_e is the equilibrium uptake (mg·g^{-1}), C_e is the equilibrium metal ions concentration (mg·L^{-1}), K_f (L·g^{-1}) and n are Freundlich constants. Q_o (mg·g^{-1}) is the maximal adsorption capacity and b (L·g^{-1}) is the sorption equilibrium constant. Q_{max} is the capacity of saturation theory (mg·g^{-1}), K_{ads} is the constant of adsorption energy (J^2·mol^{-2}) and ε is the potential Polanyi defined by:

$$\varepsilon = RT \log (1 + 1/C_e) \tag{6}$$

where R is the gas constant (8.314 J·mol^{-1}·K^{-1}) and T is the absolute temperature. On the other hand, the value of adsorption energy (E_a) indicating the nature of adsorption has been determined through the equation:

$$E_a = (2 \, K_{ads})^{-1/2} \tag{7}$$

2.6. Thermodynamic study

The thermodynamic study of the uranyl adsorption onto the 4A and P1 aluminosilicates consisted primarily of determining the Gibbs free energy $\Delta G°_{ads}$ of the process by means of the following well-known equation:

$$\Delta G°_{ads} = \Delta H°_{ads} - T \, \Delta S°_{ads} \tag{8}$$

The thermodynamic properties, the enthalpy $\Delta H°_{ads}$ and the entropy $\Delta S°_{ads}$ were determined through the plot and the linearization of $\ln K_d$ against $1/T$ using the combined Van't Hoff equation:

$$\ln K_d = \Delta S°_{ads}/R - \Delta H°_{ads}/RT \tag{9}$$

The distribution coefficient K_d (ml/g) is obtained as:
$$K_d = (C_i - C_{eq})V/m \, C_{eq} \text{ (mL/g)} \tag{10}$$
where $\Delta G°_{ads}$ is the adsorption standard Gibbs free energy of adsorption in kJ·mol^{-1}, $\Delta H°_{ads}$ and $\Delta S°_{ads}$ are the adsorption standard enthalpy and entropy of adsorption in kJ·mol^{-1} and kJ·mol^{-1}·K^{-1}, respectively.

2.7. UO_2^{2+} ion diffusion study

The UO_2^{2+} ion diffusion onto 4A and P1 zeolites was studied and the diffusion coefficients during the adsorption process were determined. The Fick's second law: $\partial C/\partial t = \Delta C$, written originally in Cartesian coordinates, was converted into polar spherical coordinates and finally resolved with the use of Fick's first law. The final equation, which deals with our experimental data, can be written as follows:

$$\frac{q_t}{q_\infty} = 1 - \frac{6}{\pi^2} \sum_{n=1}^{\infty} \frac{1}{n^2} exp\left(-\frac{D \, n^2 \pi^2 \, t}{r_0^2} \right) \tag{11}$$

where q_t and q_∞ are the uranium (VI) adsorbed quantities at time t and to infinity, n is an integer, r_0 is the zeolite particle radius and D is the diffusion coefficient.

The application of the equation (11) to the short-time-occurred processes and considering the zeolite grains as spherical isotropic particle with radius r_0, Eq. (11) becomes then:

$$\frac{q_t}{q_e} = \frac{6}{r_0} \left(\frac{D \, t}{\pi} \right)^{0.5} \tag{12}$$

The adsorption capacity to infinity, q_∞, is replaced by a more practical equilibrium adsorption capacity q_e.

The activation energies of the diffusion, E_{dif} (kJ·mol^{-1}), of uranyl ions onto 4A and P1 zeolites were determined by means of Arrhenius equation applied to the adsorption process:

$$\ln D = \ln D_0 - \frac{E_{diff}}{RT} \tag{13}$$

where D is the diffusion coefficient (or diffusivity) in m^2·s^{-1}, D_0 is the maximum diffusion coefficient (at infinite temperature), T is the temperature in K, and R is the gas constant.

Similarly, the activation entropy was determined through Arrhenius equation applied to the diffusion:

$$D_0 = \left[\frac{2.72KTd^2}{h} \right] \exp(\Delta S^*/R) \tag{14}$$

where K is the Boltzmann constant, h is the Planck constant, d is the distance between the active sites within the material considered, R is the gas constant, and T is the

temperature. Globally, the data of activation entropies obtained ΔS^* give an indication on the exchange reaction mechanism, whether it is an association (fixation) or a dissociation mechanism [18,19]. Accordingly, the entropy value higher than $-10\,\text{J·mol}^{-1}\text{·K}^{-1}$ indicates that the mechanism at work is dissociation.

3. Results and discussion

3.1. Determination of the adsorption equilibrium time

Uranium (VI) kinetic adsorption onto 4A and P1 zeolites was studied in the following conditions: $[UO_2^{2+}]$: $10\,\text{mg·L}^{-1}$, S/L ratio: 1/100, T: 293 K, and pH: 2 (4A) and 2.5 (P1). The results are shown in Fig. 3, where the representative curve of the phenomenon consists of two distinct phases. The uranium adsorbed reached a maximal value at a stirring time $t = 60$ min. However, the optimal equilibrium time of 120 min was retained and used in the subsequent experiments.

3.2. Effect of pH

The influence of the pH on the adsorption of the uranyl ions onto 4A and P1 zeolites was studied in the following conditions: $[UO_2^{2+}]$: $10\,\text{mg·L}^{-1}$, S/L ratio = 1/100, T: 293 K, and contact time: 120 min, in a pH range from 2 to 11 (Fig. 4). The pH of the solution was adjusted using KOH and HCl solutions. The aqueous solution pH seems to be an important factor for controlling the process of uranium adsorption on aluminosilicates [1,3,20]. The adsorption percentage has been found maximal at pH = 2 onto 4A and at pH = 2.5 onto P1; this is mainly due to the hydrolysis of the uranyl ion and to its freedom, which means that there was no precipitated uranyl species present, and hence that adsorption was improved. However, with increasing pH, the complexes form with the prevalent uranium species $(UO_2(OH)^+, (UO_2)_2(OH)_2^{2+}, (UO_2)_3(OH)_5^{3+}$ and $(UO_2)_2(OH)_2)$, preventing adsorption [19].

Fig. 4. Effect of pH on uranium (VI) adsorption onto 4A and P1 zeolites. ($[UO_2^{2+}] = 10\,\text{mg·L}^{-1}$, $t = 2$ h, $S/L = 1/100$ and $T = 293$ K).

3.3. Effect of uranium (VI) initial concentration

Uranium (VI) adsorption onto 4A and P1 zeolites was studied as a function of the initial uranyl concentration, which was varied in the range from 5 to $100\,\text{mg·L}^{-1}$. The prevailing experimental conditions were: the ambient temperature, solid–liquid ratio = 1/100, contact time = 120 min, pH = 2 and 2.5 for 4A and P1 zeolites, respectively. The results are shown in Fig. 5. It can be seen from this figure that the adsorbed uranium percentage decreases with increasing the initial concentration; this is mainly due to the higher mobility of the UO_2^{2+} ion in diluted solutions and therefore to its higher interaction with the adsorbent.

3.4. Effect of temperature

In order to study the influence of the temperature on the uranyl ion adsorption yield, a set of batch experiments were performed over the temperature range from 293 to 343 K. The results are shown in Fig. 6, where we notice that
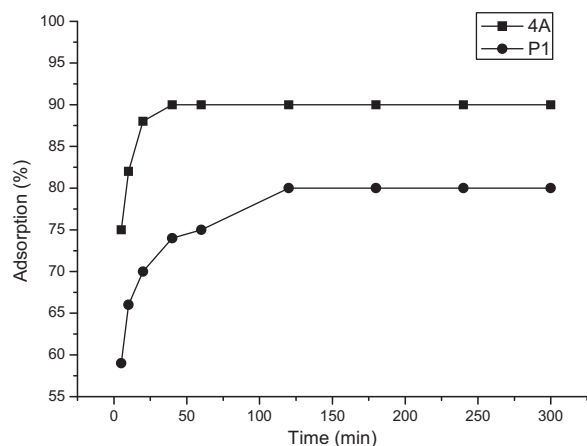

Fig. 3. Effect of contact time on uranium (VI) adsorption onto 4A and P1 zeolites ($T = 293$ K, $[UO_2^{2+}] = 10\,\text{mg·L}^{-1}$, pH (4A) = 2, pH (P1) = 2.5 and $S/L = 1/100$).
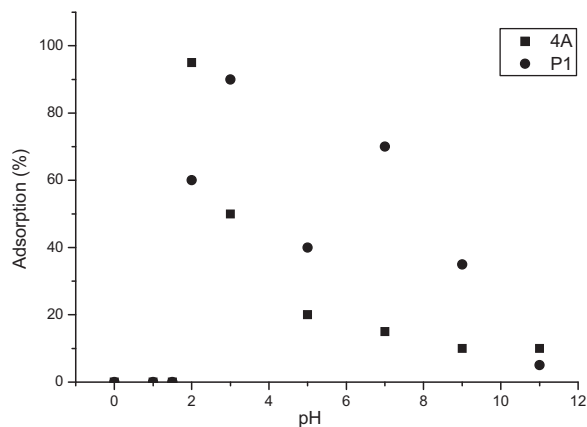

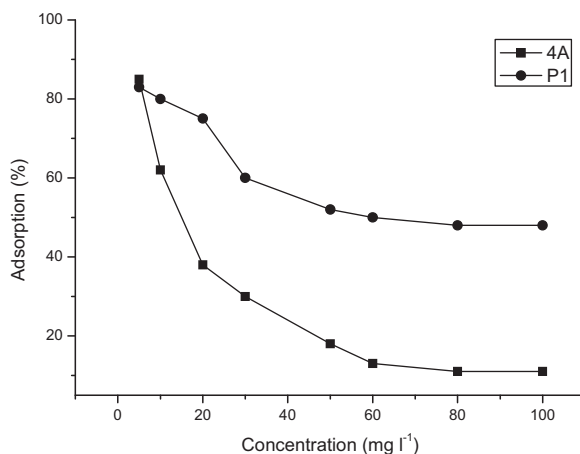**Fig. 5.** Influence of initial concentration on uranium (VI) adsorption onto 4A and P1 zeolites [$T = 293$ K, pH (4A) = 2, pH (P1) = 2.5, $S/L = 1/100$ and $t = 2$ h].

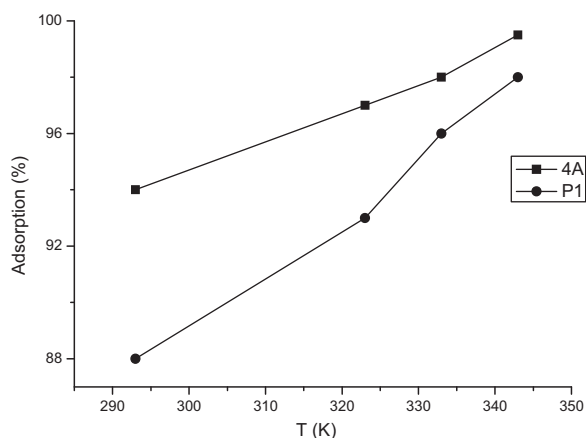**Fig. 6.** Effect of temperature on uranium (VI) adsorption onto 4A and P1 zeolites. ($[UO_2^{2+}] = 10$ mg·L^{-1}, pH (4A) = 2, pH (P1) = 2.5, S/L = 1/100 and t = 2 h).

Fig. 7. Pseudo second-order kinetic plots for uranium (VI) adsorption onto 4A and P1 zeolites (T = 293 K, $[UO_2^{2+}] = 10$ mg·L^{-1}, pH (4A) = 2, pH (P1) = 2.5 and S/L = 1/100).

the temperature increase improved the adsorption process. In fact, the adsorption uranium (VI) percentage onto 4A and P1 zeolites reached 99% and 97%, respectively, at the temperature of 343 K. The process is therefore endothermic. This result is similar to that reported by Kütahyah et al. [21] in their study on uranium and thorium sorption on activated carbon.

3.5. Adsorption dynamic of uranium (VI) onto 4A and P1 zeolites

The kinetic adsorption experimental study of uranium (VI) onto 4A and P1 zeolites has been carried out under the following conditions: ambient temperature, pH = 2.5, initial concentration 10 mg·L^{-1} and solid/liquid ratio R = 1/100.

The adsorption rate constants for all the models used, namely the pseudo first- and second-order, the intraparticle diffusion, were determined by linear regression of the data obtained experimentally. The results are shown in
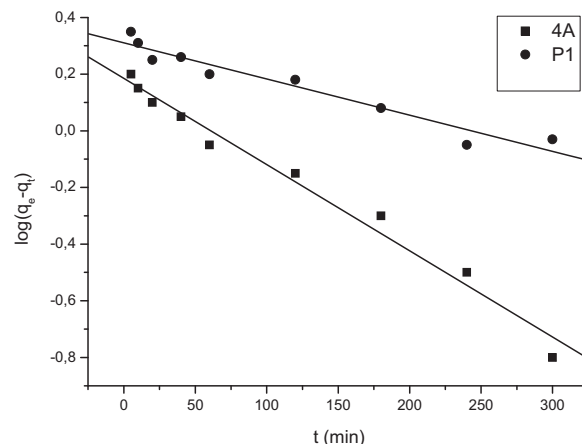
Fig. 7 and the figures representing the rate constants are compiled in Table 2. We notice that the adsorption is the fastest under the pseudo first-order model, which accurately fits well the experimental data. Wang et al. [22] suggested that adsorption of uranium (VI) on modified clay followed better the pseudo second-order model. In the case of clay, the interaction is mainly electrostatic.

3.6. Study of the uranium adsorption equilibrium

The equilibrium adsorption isotherms are important for investigating the adsorption capacity of UO_2^{2+} onto 4A and P1 zeolites, and the type of adsorption. The different characteristic coefficients data obtained, concerning the models used: Langmuir, Freundlich and Dubinin–Raduchkevitch constants as well as the corresponding correlation coefficients are given in Table 3. According to these data, it emerges that the Langmuir model fits best the results of our adsorption experiments; the isotherms for 4A and P1, respectively, are displayed in Fig. 8. The adsorption energy

Table 2
Kinetic parameters for the adsorption of uranium (VI) onto 4A and P1 zeolites (T = 293 K, $[UO_2^{2+}] = 10$ mg·L^{-1}, pH (4A) = 2, pH (P1) = 2.5 and S/L = 1/100).

Zeolites	Pseudo first-order				Pseudo second-order				Intra particle diffusion	
	q_e (cal) (mg g^{-1})	k_{1ads} (min^{-1})	R^2	q_e (cal) (mg g^{-1})	k_{2ads} (g mg^{-1}·mn^{-1})	h (mg g^{-1}·min^{-1})	R^2	q_e (exp) (mg g^{-1})	K_p (mg g^{-1} mn$^{-0.5}$)	R^2
4A	1.078	4.37×10^{-2}	0.995	10.03	5.85×10^{-2}	5.865	0.993	0.912	8.79×10^{-2}	0.558
P1	2.146	3.45×10^{-3}	0.976	9.33	1.12×10^{-1}	9.750	0.961	2.373	10.41×10^{-2}	0.422

Table 3
Values of the Langmuir, Freundlich and Dubinin–Radushkevich (D–R) constants for the adsorption of uranium (VI) species onto 4A and P1 zeolites (T = 293 K, pH (4A) = 2, pH (P1) = 2.5 and S/L = 1/100).

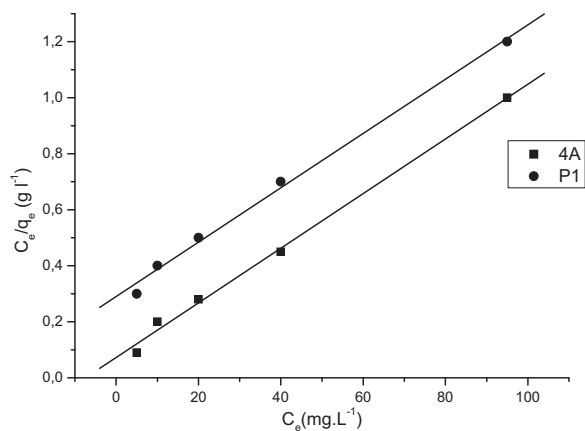| Zeolites	Langmuir				Freundlich			Dubinin–Radshkevich (D–R)			
	Q_0 (mg·g^{-1})	b (L·g^{-1})	R_L	R^2	n	k_f (L·g^{-1})	R^2	Q_{max} (mg·g^{-1})	k_{ads}	R^2 (J^2·mole^{-2})	E_a (mg·g^{-1})
4A	1	2.4×10^{-4}	0.112	0.997	6.54	0.5	0.943	1.60	15.6×10^{-9}	0.876	22.36
P1	3.72	1.6×10^{-4}	0.134	0.984	2.10	0.63	0.953	21.63	8.9×10^{-9}	0.890	11.18

Fig. 8. Langmuir isotherm for uranium (VI) adsorption onto 4A and P1 zeolites [T = 293 K, pH (4A) = 2, pH (P1) = 2.5 and S/L = 1/100].

(E_a) calculated from the constant of adsorption energy (K_{ads}) is useful for estimating the type of adsorption reaction. If the value of E_a is less than 8 kJ·mol^{-1}, the nature of adsorption is physical. But if it ranges between 8 and 25 kJ·mol^{-1}, the adsorption is an ion exchange [23–25]. In the present case and from the data in Table 3, the E_a values for 4A and P1 zeolites indicate clearly an ion exchange mechanism.

The Langmuir parameters were used to calculate the R_L factor; this coefficient represents the affinity between the material and the adsorbate. The effect of the initial uranyl concentration on the R_L factor was studied and the data are shown in Fig. 9. It is clear from these results that the affinity that is referred to is more important for high initial uranium (VI) concentrations. Moreover, R_L data between 0 and 1 suggest that the adsorption is favoured [19,26].

3.7. Uranyl ion UO$_2^{2+}$ diffusion study

In order to determine the uranyl ion diffusion coefficients during the adsorption process onto 4A and P1 zeolites, the Fick's laws of diffusion were used [1,18].
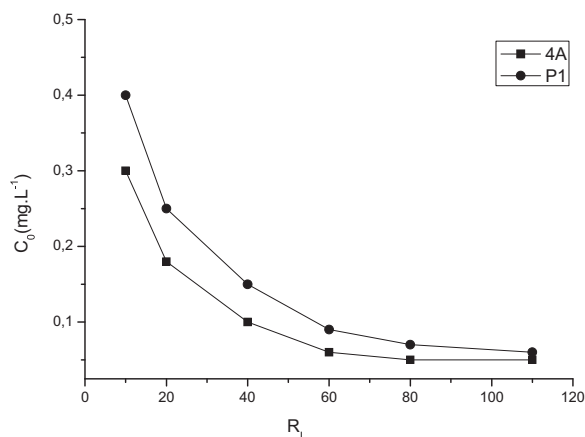

Fig. 9. Separation factor R_L for uranium (VI) adsorption onto 4A and P1 zeolites [T = 293 K, pH (4A) = 2, pH (P1) = 2.5 and S/L = 1/100].
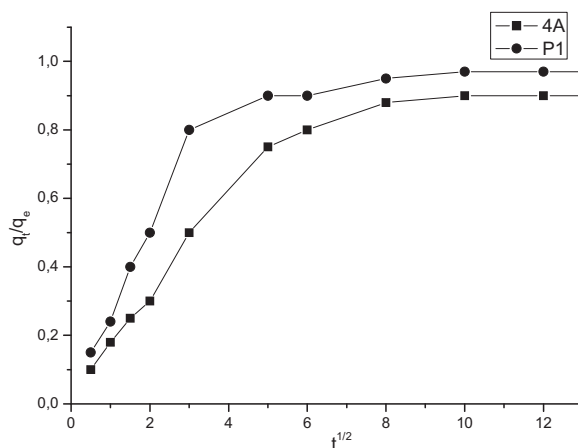

Fig. 10. q_t/q_e vs. $t^{1/2}$ plots of the early stage of the adsorption of uranium onto 4A and P1 zeolites (T = 293 K, [UO$_2^{2+}$] = 10 mg·L^{-1}, pH (4A) = 2, pH (P1) = 2.5 and S/L = 1/100).

The plot of the quantity (q_t/q_e) against $t^{1/2}$ (Fig. 10) and after linear regression were drawn, the diffusion coefficients D_i were determined; they have been found to be 1.36×10^{-12} and 0.075×10^{-12} m^2/s for zeolites 4A and P1, respectively. These results indicate that uranyl ions diffuse better in 4A zeolite, which can be explained by the difference in the chemical composition, the cations' distribution, the Si/Al atoms ratio in the zeolite tetrahedron and the pores aperture (4A: 4×4 Å and P1: 4.5×3.1 Å). The diffusion activation energies were calculated from the plot of ln D versus $1/T$; the values are compiled in Table 4. We notice that the activation energy of diffusion (E_{dif}) onto P1 is smaller than that onto 4A, indicating that uranyl ion UO$_2^{2+}$ diffuses more easily through the pores of zeolite 4A, whose porous volume is larger than that of P1 (0.16 mL·g^{-1} and 0.17 mL·g^{-1}). In order to explain and to understand the experimental results, Kristou et al. [7] reported that the ability of zeolite to exchange cations with a solution is strongly related to the dimensions of the channels and the size that the UO$_2^{2+}$ cations in solution have. The ionic radius of uranyl ion is equal to 1.8 Å. This size is much less than the dimension of 4A and P1 channels, indicating that uranium (VI) ions in the solution have an access to their exchangeable sites.

As for the entropy of activation (ΔS^*), the values obtained and reported in Table 4 are negative; therefore, the mechanism under which the diffusion took place is an association mechanism. The basic internal structure of the zeolites did not undergo any change. This result reflects that a good agreement was seen on 4A and P1 zeolites X-ray patterns before and after UO$_2^{2+}$ adsorption (Fig. 1b and Fig. 2b). Also, it is similar to that reported by Akyl et al. [3] in their study on the distribution of uranium on zeolite X and

Table 4
Diffusion activation energy E_{dif}, diffusion ccoefficient D_0 and activation entropy ΔS^* onto 4A and P1 zeolites.

Zeolites	E_{dif} (kJ·mol^{-1})	D_0 (m^2·s^{-1})	ΔS^* (J·mol^{-1}·K^{-1})
4A	40.376	4.58×10^{-9}	−49.684
P1	25.289	1.37×10^{-14}	−89.123

Table 5
Thermodynamic parameters for uranium (VI) adsorption onto 4A and P1 zeolites.

Zeolites	ΔH°_{ads} (kJ·mol^{-1})	ΔS°_{ads} (J·mol^{-1}·K^{-1})	ΔG°_{ads} (kJ·mol^{-1})			
			293 K	303 K	313 K	323 K
4A	39.14	112.95	−17.42	−23.18	−25.11	−27.04
P1	24.12	136.06	−15.75	−19,82	−21.18	−22.16

investigation of the thermodynamic parameters for this system.

3.8. Thermodynamic study

The resolution of the Van't Hoff equation by plotting ln K_d against $1/T$ [1,24] led to the determination of the adsorption enthalpy and entropy ΔH°_{ads} and ΔS°_{ads} through linear regression, the results are shown in Table 5. The positive values of the adsorption enthalpy indicate that the uranium (VI) adsorptions onto 4A and P1 zeolites are endothermic processes, which is also indicating by increasing adsorption with increasing temperature. The negative Gibbs free energy values prove the feasibility as well as the spontaneity of the adsorption.

3.9. Experimentation on real effluents

The following step of our work consisted in testing 4A and P1 zeolites in genuine solutions. A set of experiments was carried out at the adsorption optimum conditions previously obtained in the study of the synthetic solutions.

The effluents were taken at different points along the process of uranium purification and concentration in the uranium ore treatment. The yellow cake, which is a mixture of oxides whose composition is expressed in U_3O_8, is the first uranium compound produced at this stage of uranium ore refining; it is then sent and used as a raw material in the purification process, where it is converted into a more concentrated compound called ammonium diuranate (ADU) or ammonium uranyl carbonate (AUC). The processes that is referred to concern different unit operations such as extraction, re-extraction, washing, precipitation; generating several effluents that need to be treated. In this respect, three solutions with initial

Table 6
Experimental data on radioactive waste treatment by adsorption onto 4A and P1 zeolites.

Zeolite	Solution 1 (100 mg·L^{-1})	Solution 2 (85 mg·L^{-1})	Solution 3 (80 mg·L^{-1})
	Uptake uranium adsorption		
4A Condition pH: 2 T: 343 K	96.66	96.31	98.12
P1 Condition pH: 2.5 T: 343 K	90.82	90.60	91.61

concentrations of 100, 85 and 80 mg·L^{-1} were used. The results are shown in Table 6; it emerges that our zeolites 4A and P1 effectively removed uranyl ion UO_2^{2+} with a yield higher than 96%.

4. Conclusion

In the present comparative study, the ability of two locally produced zeolites, namely 4A and P1, were tested for the adsorption of uranyl ion UO_2^{2+} in aqueous solutions.

Both zeolites (4A and P1) were synthesized and characterized. The equilibrium time was determined and found to be 60 min under the following condition: $T = 293$ K, pH = 2.0 and 2.5 for 4A and P1, respectively, initial uranium (VI) concentration $C_0 = 100$ mg·L^{-1}, and a solid–liquid ratio = 1/100. However, the optimal operating time taken by the subsequent experiments was 120 min. The effect of the parameters that are referred to on the adsorption yield was studied. The two zeolites adsorb effectively uranium (VI) and pH is the most important parameter. The maximal adsorption yield was obtained at pH = 2.0 for zeolite 4A and 2.5 for the zeolite P1.

Our experimental data fit best the pseudo first-order, with a correlation coefficient of nearly one, and our equilibrium adsorption capacities q_e (cal) are close to the experimental ones q_e (exp) for both zeolites produced. As for equilibrium, the Langmuir model was found to describe best our experimental results for both zeolites. It is also shown that the adsorption capacity onto P1 is higher than onto 4A. Besides, the figures obtained for the dimensional factor $0 < R_L < 1$ indicate that the adsorption is favourable.

The low values of the diffusion activation energy E_{dif} showed that the uranyl ion diffuse easily through the zeolites 4A and P1 pores. The negative values of the Gibbs free energy showed clearly the feasibility of the adsorption phenomenon; however, adsorption is more possible onto zeolite 4A ($\Delta G^\circ_{ads} = -27.04$ kJ·mol^{-1}) than onto P1 ($\Delta G^\circ_{ads} = -22.16$ kJ·mol^{-1}). The standard adsorption entropies and enthalpies were found to be positive, indicating that the adsorption onto our two zeolites is spontaneous and endothermic.

Eventually, a set of adsorption experiments were conducted onto our locally made zeolites 4A and P1 with a genuine low-level radioactive effluent. The results are encouraging, as the adsorption yield reached exceeds 96%. In conclusion, the different results obtained suggest a chemical nature of the adsorption (chemisorptions), which makes its recycling hard.

References

[1] D. Nibou, S. Khemaissia, S. Amokrane, M. Barkat, S. Chegrouche, A. Mellah, Chem. Eng. J. 172 (2011) 296–305.

[2] S. Khemaissia, Synthesis and characterization of zeolite materials and their use in the radioactive waste processing (Ph.D thesis), University of Science and Technology Houari Boumediene, Algiers, Algeria, 2008.

[3] S. Akyıl, A. Mahmoud, A. Aslani, J. Alloys Compds. 271/273 (1998) 769–773.

[4] M. Barkat, Study and characterization of natural porous materials. Valorization in liquid effluent treatment (Ph.D thesis), University of Science and Technology (USTHB), Algiers, Algeria, 2010.

[5] E.R. Sylvester, E.A. Hudson, P.G. Allen, Geochim. Cosmochim. Acta 64 (14) (2000) 2431–2438.

[6] A. Mellah, S. Chegrouche, M. Barkat, J. Colloid Interf. Sci. 296 (2) (2006) 434–441.
[7] A. Krestou, A. Xenidis, D. Panias, Min. Eng. 16 (2003) 1363–1370.
[8] D. Nibou, S. Amokrane, C. R. Chimie 13 (5) (2010) 527–537.
[9] S. Amokrane, D. Nibou, C. R. Chimie 13 (5) (2010) 538–543.
[10] A. Dyer, An Introduction to Zeolite Molecular Sieve, John Wiley, London, 1988.
[11] S. Amokrane, R. Rebiai, S. Lebaili, D. Nibou, G. Marcon, Stud. Surf. Sci. Catal. Ser. 135 (2001) 230.
[12] D.W. Breck, Zeolites molecular sieves-structure, chemistry and use, Wiley-Interscience, New York, 1974.
[13] D. Nibou, S. Amokrane, H. Mekatel, N. Lebaili, Phys. Proc. 2 (2009) 1433–1440.
[14] J.C. Jansen, in: H. Van Bekkum, E.M. Flanigen, P.A. Jacobs, J.C. Jansen (Eds.), Introduction to zeolite science and practice, 2nd Ed., Elsevier, Amsterdam, 2001.
[15] Ch. Baerlocher, W.M. Meir, D.H. Olson, Atlas zeolites Framework Types, Fourth Revised ed, Elsevier, Amsterdam, 2001.
[16] M.M.J. Treacy, J.B. Higgins, Collection of Simulated XRD Powder Paterns for Zeolites, Fourth Revised ed, Elsevier, Amsterdam, 2001.
[17] J. Vesley, D. Weiss, K. Stulik, Analysis with Ion Selective Electrodes, Wiley Interscience, New York, 1978.
[18] D. Nibou, H. Mekatel, S. Amokrane, M. Barkat, M. Trari, J. Hazard. Mater. 173 (2010) 637–646.
[19] S. Olmez Aytas, S. Akyil, M. Eral, J. Radio. Nucl. Chem. 260 (1) (2004) 119–125.
[20] D. Nibou, Elaboration and characterization of solid microporous materials (Ph.D thesis), University of Science and Technology (USTHB), Algiers, 1999
[21] C. Kütahyah, M. Eral, J. Nucl. Mater. 39 (2010) 251–256.
[22] G. Wang, X. Wang, X. Chaia, J. Lieu, N. Deng, Appl. Clay Sci. 47 (3–4) (2010) 448–451.
[23] M. Barkat, D. Nibou, S. Chegrouche, A. Mellah, Chem. Eng. Proc. 48 (1) (2009) 38–47.
[24] A. Krobba, D. Nibou, S. Amokrane, H. Mekatel, Desalin. Water Treat. 37 (2012) 31–37.
[25] J. Warchoł, M. Matłok, P. Misaelides, F. Noli, D. Zamboulis, A. Godelitsas, Micropor. Mesopor. Mater. 153 (2012) 63–69.
[26] A. Houhoune, D. Nibou, S. Amokrane, M. Barkat, Desalin. Water Treat. 51 (28–30) (2013) 5583–5591.